Available online at www.sciencedirect.com
ScienceDirect
Journal of Chromatography B, 855 (2007) 186–199
JOURNAL OF CHROMATOGRAPHY B
www.elsevier.com/locate/chromb

Radical peroxidation of palmitoyl-lineloyl-glycerophosphocholine liposomes: Identification of long-chain oxidised products by liquid chromatography–tandem mass spectrometry

Ana Reis, M.R.M. Domingues, F.M.L. Amado, A.J. Ferrer-Correia, P. Domingues *

Department of Chemistry, University of Aveiro, 3810-193 Aveiro, Portugal

Received 25 December 2006; accepted 1 May 2007
Available online 17 May 2007

Abstract

Liquid chromatography coupled with electrospray tandem mass spectrometry (LC–MS/MS) was used to identify palmitoyl-lineloyl-glycerophosphatidylcholine oxidation products (PL(O_{1-6})PC). Structural and positional isomers of keto, hydroxy and/or epoxy, and hydroperoxide derivatives of PLPC were identified based on MS/MS data, namely product ions attributed to lyso-phosphatidylcholines, product ions formed by loss of $n H_2O$ and H_2O_2 from $[MH]^+$ ions groups, and product ions involving the hydroxy groups, providing information about the position of these groups and of the double bonds along the carbon chain of lineloyl moiety.

Keywords: Phospholipids; Glycerophosphatidylcholine; Oxidation; LC–MS/MS

1. Introduction

Free radicals formed within the cell during aerobic processes are generally trapped by enzymatic and/or non-enzymatic antioxidant systems [1]. However, when an imbalance between the radicals formed and the antioxidant systems occurs oxidative damage takes place. For this reason, in recent years, oxidative damage to biomolecules by free radicals has received increasing attention due to the growing evidence of its involvement in many age-related diseases, such as atherosclerosis, Alzheimer, Parkinson, multiple sclerosis, and some liver and lung diseases [1]. The oxidative damage to biomolecules, which is caused by the high reactivity of free radicals towards unsaturated compounds such as DNA bases, amino acid residues and polyunsaturated fatty acids (PUFA) [2], is mostly focused on the structural changes induced to peptides and proteins. On the other hand, phospholipids, present in cell membranes, low-density lipoproteins (LDL), cholesterol and triglycerides [2], playing an important role in membrane structure, metabolism and signal transduction [3], are also major targets of free radicals and have not been so extensively studied. Nonetheless, from the works published it has been inferred that the structural changes caused by radical peroxidation in phospholipids, such as phosphatidylcholines, affect the physical properties of the membrane bilayers [4,5] which are reflected in membrane integrity [6]; and are also responsible for covalent cross-linking between oxidised lipid moieties and proteins [7,8] leading to inactivation of membrane proteins and/or receptors [9]. In some cases, oxidised phospholipids show biological activity similar to platelet aggregating factors (PAF) [10], or may act as promoters in the expression of several genes, as proposed in the tumorogenesis of breast cancer cells [11].

Mass spectrometry (MS), using both electrospray (ES) and matrix-assisted laser ionisation (MALDI) methods, and applied to the screening of phospholipid classes [12,13], are also used in the study of oxidised phosphatidylcholines either on the identification of short-chain products [14–16] or of long-chain products [17–20]. Because the structural changes induced by free radicals to phospholipids occur on the PUFA acyl chains esterified to the polar head, in the particular case of phosphatidylcholines, these have been identified through the characterisation of oxidised fatty acid extracts obtained by saponification, which are extrapolated to intact oxidised phosphatidylcholines [21–24], or based on the *m/z* value of the peaks observed in the mass spectra of intact oxidised phosphatidylcholines [16,17,19,25].

* Corresponding author. Tel.: +351 234 370699; fax: +351 234 370084.
E-mail address: pedrom@dq.ua.pt (P. Domingues).

1570-0232/$ – see front matter © 2007 Elsevier B.V. All rights reserved.
doi:10.1016/j.jchromb.2007.05.006

In the case of long-chain products, the increase of oxygen atoms inserted into the unsaturated fatty acid chains increases the structural variability (structural and positional isomers), which is often observed with the increase of the number of peaks in chromatography experiments [19,20,25,26]. As consequence, the identification of these products is complex and is best achieved through LC coupled with MS/MS. The knowledge about the structure of phospholipid peroxidation products is even more relevant as oxidised phosphatidylcholines are being considered as potential biomarkers [27,28] after the concentration of phosphatidylcholine hydroperoxide (PCOOH) was found to be significantly higher in the plasma of patients with blood alcohol when compared with controls [28]. To our knowledge, attempts made on the analysis of the oxidised long-chain phosphatidylcholine products itself by LC–MS/MS were recently reported, in which the authors have identified oxo, hydroxy, hydroperoxide and tri-hydroxy derivatives of PLPC based on the presence of the product ions due to loss of water molecules from the precursor ion [26,28]. No further structural information, regarding the location of the proposed substitutents along the unsaturated carbon chain, were made by the authors.

In this work, we present and discuss the results obtained by liquid chromatography coupled with electrospray tandem mass spectrometry (LC–MS/MS) of radical oxidised long-chain palmitoyl-lineloyl-glycerophosphatidylcholine (PLPC) phospholipid liposomes. Using the LC–MS/MS fragmentation patterns, namely the product ions due to loss of water and hydrogen peroxide together with other product ions attributed to cleavages in the unsaturated fatty acid chain, different peroxidation products will be identified in more detail, with focus on the formation of the different isomers, as the result of glycerophosphatidylcholine (GPC) radical oxidation.

2. Experimental

2.1. Preparation and oxidation of GPC vesicles

Vesicles were prepared from stock solutions of 1 mg/mL of phospholipids in ammonium bicarbonate buffer (5 mM, pH 7.4) to a final phospholipid concentration of 50 mM. Oxidative treatments performed on the GPC vesicles were done as described elsewhere [25]. Briefly, oxidative treatments using Fe(II) and hydrogen peroxide (H_2O_2) were carried out by adding to 50 μL of phospholipid vesicles, 5 mmol $FeCl_2$ solution and 50 mmol of H_2O_2 in 0.5 mL solution. This mixture was left to react at 37 °C in the dark for 24 h with occasional sonication. The phospholipid oxidation products were extracted using the Folch method with chloroform:methanol (2:1, v/v) [29].

2.2. Liquid chromatography–electrospray mass spectrometry (LC–MS and LC–MS/MS)

The HPLC-MS study was performed with a Waters Alliance (Milford, USA) Model 2690 equipped with an APEX 300 C4 column 7 μm (250 mm × 4.6 mm I.D., Jones Chromatography) attached to the mass spectrometer. The reaction mixture (50 μL) was introduced into the column, kept at 30 °C, and the peroxidation products separated using the gradient of aqueous ammonium acetate (5 mM):acetonitrile (90:10, v/v) (eluent A) and acetonitrile:aqueous ammonium acetate (5 mM) (90:10, v/v) (eluent B) programmed as follows: 60% B for 30 min followed by a linear increase to 100% B at 33 min held for 5 min. After 38 min, the mobile phase composition was returned to the initial conditions (5 min) for column re-equilibration (15 min). The flow rate through the column was 0.8 mL min^{-1} and it was redirected to the mass spectrometer by a capillary of 70 cm (0.350 mm × 0.150 mm) length with a flow of 50 μL min^{-1} using a home made split.

The Q-TOF2 (Micromass, Manchester, UK) mass spectrometer using a MassLynx software system (version 4.0) was operated in the positive ion mode with a capillary voltage of 3 kV, the cone voltage of 30 V, the source block temperature set to 100 °C and the desolvation temperature set to 200 °C. Mass spectra were obtained over a mass range of *m/z* 100–1200. The LC–MS/MS experiments were performed by selecting the precursor ion of interest using Q1, and collisionally, inducing fragmentation using argon as the collision gas. The collision energy varied according to the ion of interest (between 25 and 35 eV). For accurate mass measurements of each of the ion species studied, the lock mass in each product ion mass spectrum was the calculated monoisotopic mass/charge ratio of the precursor ion.

3. Results and discussion

Long-chain PLPC products resultant from radical oxidation were observed as $[MH]^+$ ions at *m/z* 774.6, 790.6, 806.6, 822.6, 838.6 and 854.6 [25] and identified as peroxidation products resulting from the insertion of one to five oxygen atoms into the *sn*-2 unsaturated fatty acid chain of the linoleic acid [25], since the palmitic acid (saturated fatty acid as *sn*-1 residue) is resistant to radical oxidation [30]. Ions exhibiting the same *m/z* values have been reported to occur in stress conditions using radiation-induced peroxidation of PLPC liposomes [19]. The reconstructed ion current (RIC) chromatogram obtained for each of these ions was plotted (Fig. 1) showing a change in the elution behaviour of the different peroxidation products. Also, other peroxidation products observed in the LC–MS spectrum at *m/z* 772.6, 788.6, 804.6, 820.6 and 836.6, exhibiting 2 Da mass decrease relative to the previous ions, resulted from the insertion of oxygen atoms and were attributed to $[MH]^+$ ions of the keto, keto-hydroxy, keto-hydroperoxy and keto-poly-hydroxy derivatives, while ions with *m/z* 808.6, 824.6 and 840.6, exhibiting 2 Da increase relative to the ions with *m/z* 806.6, 822.6 and 838.6, were only observed for the peroxidation products containing three or more oxygen atoms. The RIC chromatograms obtained for each of these derivatives were plotted (Fig. 2) showing different elution times suggesting the contribution of peroxidation products with different structural features for the same number of oxygen atoms. Oxo PLPC derivatives (*m/z* 772.6, 788.6 and 804.6) have already been identified in oxidised LDL [14,15]. In order to obtain structure elucidation of the various products formed and observed in the LC–MS chromatogram, the LC–MS/MS spectra of the major ions were obtained and will be discussed in the following sections and used for structure

elucidation. The ions with *m/z* 804.6, 820.6, 836.6, 838.6, 840.6 and 854.6 were formed with very low relative abundance, which hampered the acquisition of the product ion mass spectra.

3.1. Peroxidation products with one oxygen atom (m/z 774.6 and 772.6)

The ion at *m/z* 774.6, showed two unresolved chromatographic peaks eluting with 24.4 and 25.4 min, and a third peak eluting with 31.1 min (Fig. 1a), and the LC–MS/MS spectra obtained are shown in Fig. 3. The insertion of one oxygen atom in the linoleic acid moiety may correspond to the hydroxy or the epoxy derivatives of PLPC. The LC–MS/MS spectrum obtained for each peak and selecting the parent ion at *m/z* 774.6 (Fig. 3) showed the presence of common product ions at *m/z* 756.6 ($-H_2O$), 518.4 ($-R_1COOH$), 496.4 ($-R_2{=}C{=}O$), 478.4 ($-R_2COOH$) and 184.1 (phosphocholine head), which are characteristic losses during GPC fragmentation [31,32]. The LC–MS/MS spectrum obtained for the peak (rt 31.1 min, Fig. 3b) exhibited the product ions at *m/z* 634.5 ($-C_9H_{16}O$), 650.5 ($-C_9H_{16}$), 674.5 ($-C_6H_{12}O$) and 690.6 ($-C_6H_{12}$), resulting from losses of aldehyde and alkene molecules. The observed losses can be rationalised considering the cleavage of the C–C bond near the hydroxy group through a McLafferty-like rearrangement with hydrogen transfer [18]. These cleavages are charge-remote fragmentations and structurally informative, allowing pinpointing the hydroxy groups at C-10, C-9, C-13 and C-12, respectively (Scheme 1A–D). Previously, other authors described the product ion spectra of oxidised phosphatidylcholines obtained in QTOF instruments although product ions observed in the *m/z* range of 600–750 were not discussed [20,26]. The elemental composition determined for each product ion by accurate mass measurements (Table 1), allows to confirm the proposed structure, as can be seen for the product ion at *m/z* 650.5, $C_{33}H_{65}NO_9P^+$, showing an error of 10.1 mDa (15.5 ppm) between the observed and calculated masses. The lock mass of the product ion spectrum was calculated using the monoisotopic mass/charge of the precursor ion (*m/z* 774.5649).

The difference of 40 Da that is observed between the product ions at *m/z* 634.5 and 674.5, and also between the product

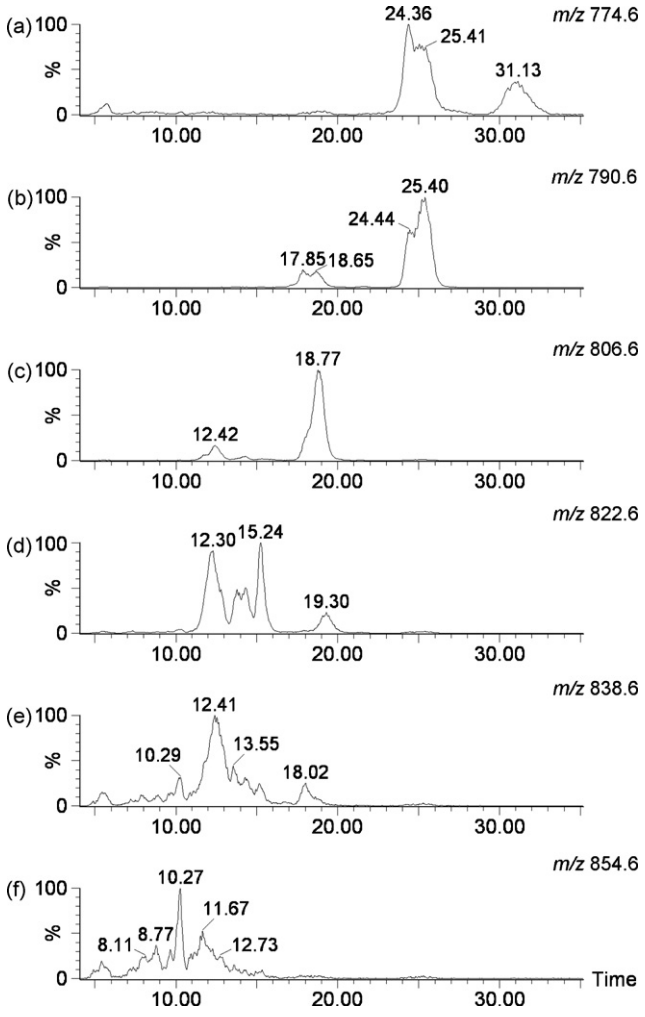

Fig. 1. Reconstructed ion chromatograms (RIC) of $[MH]^+$ ions of PLPC radical peroxidation products with *m/z* 774.6, 790.6, 806.6, 822.6, 838.6 and 854.6.

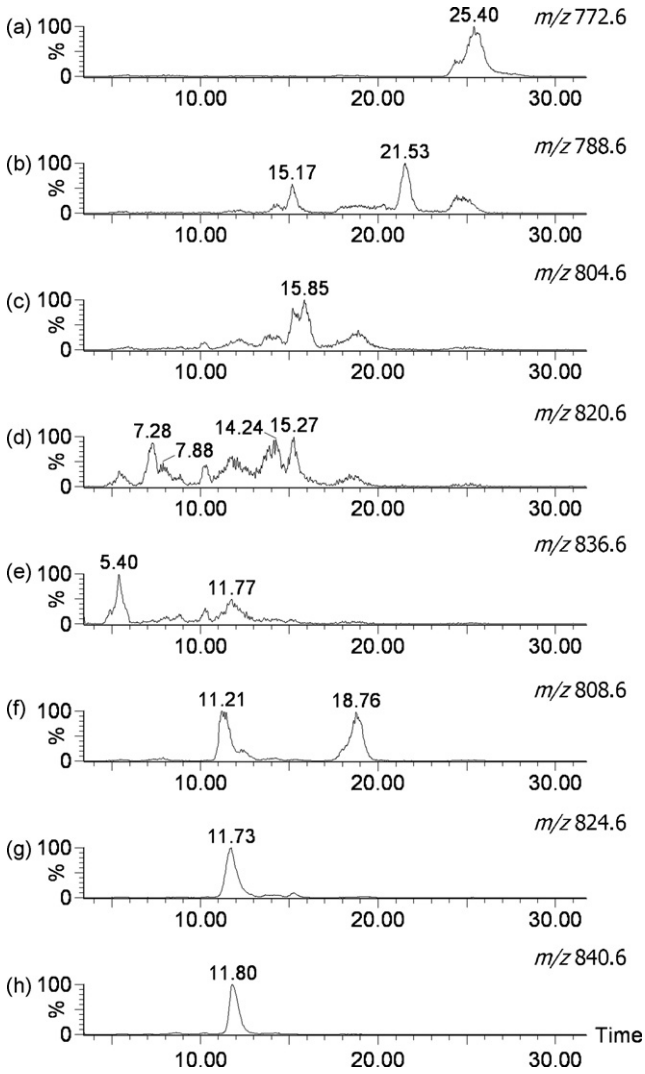

Fig. 2. Reconstructed ion chromatograms (RIC) of $[MH]^+$ ions of PLPC radical peroxidation products with *m/z* 772.6, 788.6, 804.6, 820.6, 836.6, 808.6, 824.6 and 840.6.

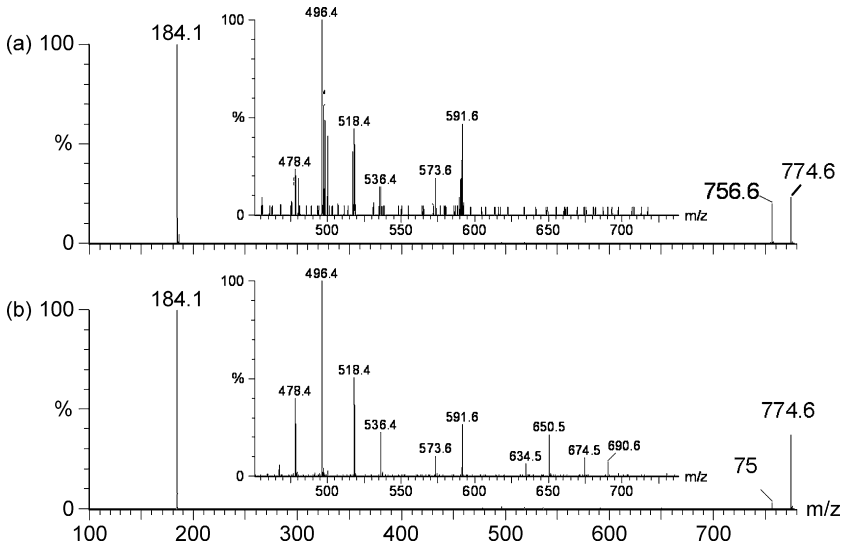

Fig. 3. LC–MS/MS spectra of $[MH]^+$ ion at *m/z* 774.6: (a) rt = 24–25 min and (b) rt = 31.1 min.

ions at *m/z* 650.5 and 690.6 is, according to Hsu and Turk [33], indicative of allylic cleavages between double bonds. Taking this into consideration, the product ions at *m/z* 650.5 and 690.5 could indicate the presence of the 7-hydroxy octadecadienoyl derivative (Scheme 1E), instead of the proposed 9-hydroxy and 12-hydroxy *sn*-2 acyl derivatives. However, for the product ions at *m/z* 634.5 and 674.5, which are also 40 Da apart, a secondary alternative structure cannot be rationalised for these product ions. For this reason, it is assumed that the product ions at *m/z* 634.5, 650.5, 674.5 and 690.6 are due to fragmentation in the vicinity of the hydroxy groups. The identification of the 9-, 10-, 12- and 13-hydroxy *sn*-2 acyl derivatives suggest that, although separation between positional isomers was not achieved under the chromatographic conditions (one peak observed in Fig. 1a), these isomers can be discriminated in a mixture through their LC–MS/MS data. This can be valuable since, for example, the 9-hydroxy derivative of PLPC was found to be elevated in erythrocyte membranes and was proposed as biomarker in diabetic patients [27].

The LC–MS/MS spectra of the ion at *m/z* 774.6 (Fig. 3a) for the peaks eluting at 24.4 and 25.4 min only showed the product ions at *m/z* 756.6 ($-H_2O$), 591.6 (–183 Da), 573.6 (–183.18 Da), 496.4 ($-R_2{=}C{=}O$) and 184.1 ($[H_2PO_4(CH_2)_2N(CH_3)_3]^+$), giving no specific structural information. Given that epoxy derivatives have already been reported as PLPC peroxidation products [20] it is proposed that these ions may correspond to epoxy derivatives of the linoleoyl moiety. Although, no fragmentation was observed under low-energy conditions used, in previous studies, epoxy fatty acid derivatives were identified and characterised under high-energy conditions, where epoxy fatty acids underwent fragmentation with cleavage in the vicinity of the epoxy ring [22,34]. Using both chromatographic and MS/MS data, and in spite of the reported instability of epoxy derivatives at 25 °C [35], both epoxy and hydroxy derivatives

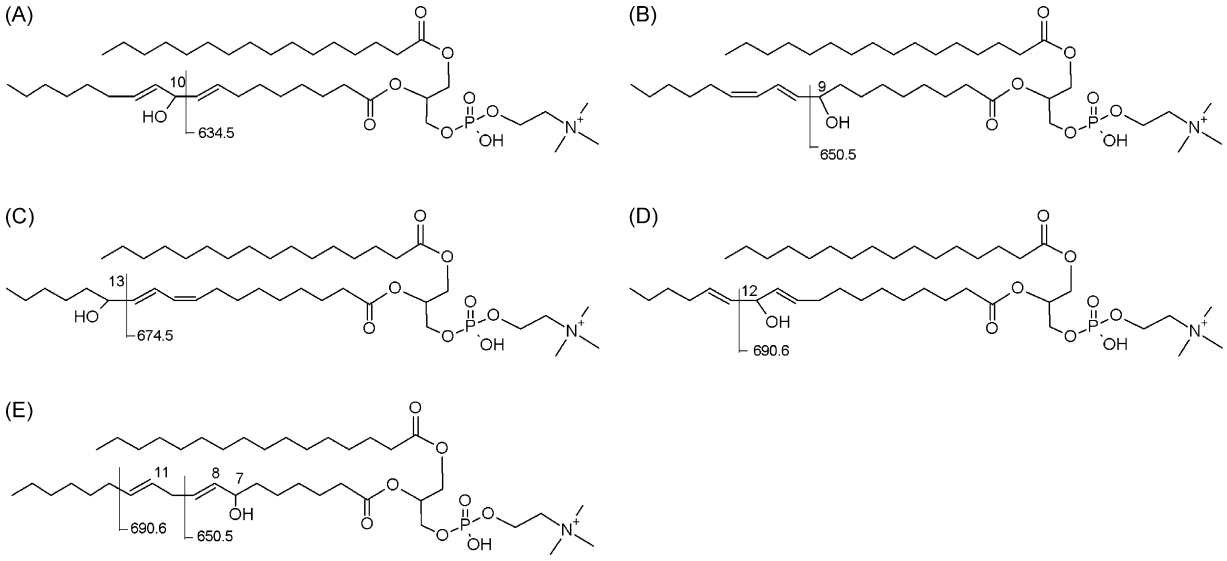

Scheme 1. Proposed structures contributing to the ion at *m/z* 774.6 (oxidation product with insertion of one oxygen atom).

Table 1
Empirical formula, observed and calculated mass/charge ratios, double bond equivalents (DBE) and mass errors of the main fragments observed in the LC–MS/MS spectra for the ion at *m/z* 774.6

Precursor ion $[MH]^+$	Product ion predicted formula	Observed mass	Calculated mass	DBE	Error (mDa)	Error (ppm)
774.6	$C_{33}H_{65}NO_8P^+$	634.4442	634.4448	2.5	−0.6	−0.9
	$C_{33}H_{65}NO_9P^+$	650.4498	650.4397	2.5	10.1	15.5
	$C_{36}H_{69}NO_8P^+$	674.4614	674.4761	3.5	−14.7	−21.8
	$C_{36}H_{69}NO_9P^+$	690.4786	690.4710	3.5	7.6	11.0

of eicosatetraenoic acid have been identified and quantified in human red blood cells, although, as stated by the authors, no statistical differences were observed for the epoxy derivatives, relative to the controls upon oxidative damage [22].

The peroxidation products identified with the suggested location for the substituting groups are summarised in Table 4. The LC–MS/MS spectrum obtained for the ion at *m/z* 772.6 (data not shown), attributed to the conjugated keto derivative eluting at 20.8 min (Fig. 2a), exhibited the product ions at *m/z* 754.6, 589.5, 534.4, 516.4, 496.4 and 478.4, together with the product ion at *m/z* 184.1 (phosphocholine head) are characteristic losses from phosphatidylcholines [31,32], and did not provide any specific structural information about the location of the keto group other than the presence of the keto group at the *sn*-2 fatty acyl chain, which is given by the 2-oxolineloyl-lyso-phosphatidylcholine product ion (*m/z* 534.4) and its dehydration product ion with *m/z* 516.4. Thus, the 9-keto-10,12-octadecadienoic acid and the 13-keto-9,11-ocatadecadienoic acid, which are the most probable oxo derivatives, are proposed as *sn*-2 acyl chains contributing to the relative abundance of the ion at *m/z* 772.6.

3.2. Peroxidation products with two oxygen atoms (*m/z* 790.6 and 788.6)

The ion at *m/z* 790.6 resulting from the insertion of two oxygen atoms in the linoleic acid moiety that may result in the formation of hydroperoxide, epoxy-hydroxy and di-hydroxy derivatives, eluted in two well separated peaks with 18 and 25 min of elution time (Fig. 1b). Each of the chromatographic peaks consisted of two other unresolved peaks with 17.8 and 18.7, and 24.4 and 25.4 min. The LC–MS/MS spectra obtained for the unresolved peaks showed no differences between them (data not shown) suggesting the presence of geometric isomers of each of the structures, thus the LC–MS/MS spectra shown in Fig. 4 were obtained for the peaks eluting with 18 and 25 min.

The LC–MS/MS spectra (Fig. 4) exhibit the product ions characteristic of $[MH]^+$ diacyl-GPC ions such as the product ions due to loss of 183 Da, loss of R_2=C=O and of R_2COOH. The product ion at *m/z* 754.6 is due to the loss of two H_2O molecules (Fig. 4a, rt 18 min) and at *m/z* 756.6 is due to loss of H_2O_2 (Fig. 4b, rt 25 min) from the precursor ion. In previous studies, by using the synthetic palmitoyl-lineloyl hydroperoxide as standard, the product ion observed due to the loss of 34 Da (H_2O_2) from the precursor ion was proposed to be indicative for the presence of the monohydroperoxide derivatives [20]. The presence of hydroperoxide derivatives was also proposed through the product ions due to loss of 32 (–O_2) from the precursor ion [18]. Nonetheless, the loss of 34 Da from the precursor ion may also be attributed to the presence of vicinal hydroxy groups, and is formed due to a combined homolytic cleavage mechanism, as proposed previously [18]. The loss of oxygen atoms in the form of water, peroxide hydrogen or oxygen prevent from obtaining structural information regarding the location of the substituting groups along the unsaturated fatty acid chain, however the product ions observed in the mass range of *m/z* 600–750 allow proposing several possible locations for the substituents.

The LC–MS/MS spectrum of the major peak at 25 min (Fig. 4b) exhibited, apart from the product ions characteris-

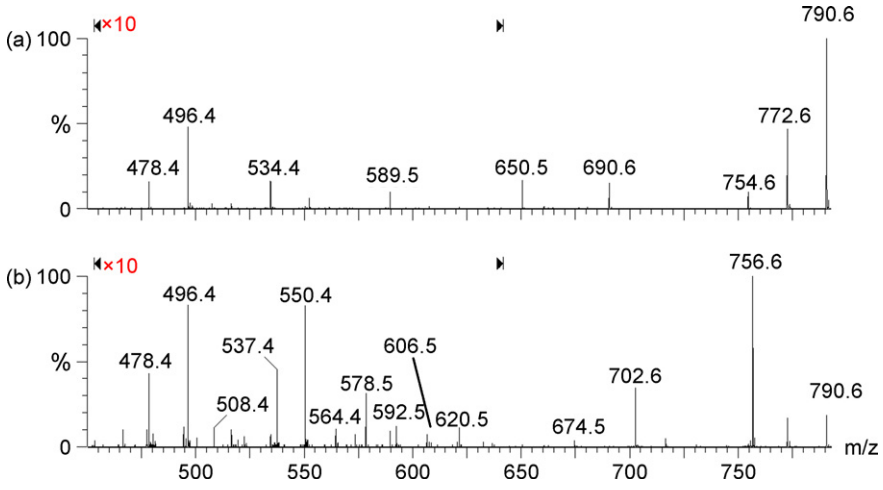

Fig. 4. LC–MS/MS spectra of $[MH]^+$ ion at *m/z* 790.6: (a) rt = 18 min and (b) rt = 25 min.

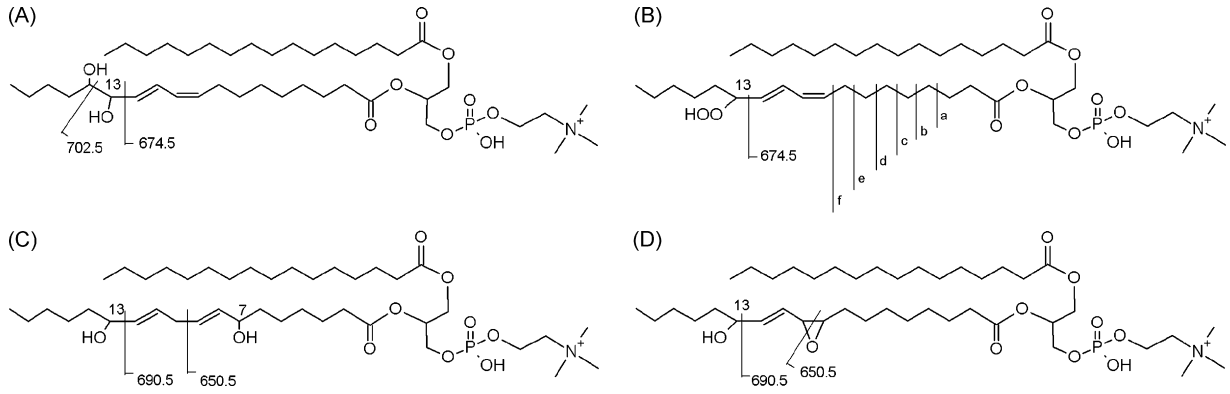

Scheme 2. Proposed structures contributing to the ion at *m/z* 790.6 (oxidation product with insertion of two oxygen atoms) showing the product ions formed by C–C cleavages.

tic of $[MH]^+$ diacyl GPC ions, the product ion at *m/z* 702.5 ($-C_5H_{12}O$) which is consistent with the presence of one hydroxy group placed at C-14, as shown in Scheme 2A. Other product ion observed at *m/z* 674.5 ($-C_6H_{12}O_2$) may result from vynillic fragmentation occurring in the same structure, suggesting the presence of the di-hydroxy derivative, placing the hydroxy groups in vicinal positions. On the other hand, the product ion at *m/z* 674.5, with the structure $C_{36}H_{69}NO_8P^+$ (Table 2), may also be assigned to the 13-hydroperoxide derivative (Scheme 2B), which would also lead to the loss of 34 Da (H_2O_2), analogous to previous published results using hydroperoxide standards [20] and of triacylglycerols [36]. These product ions are most likely resultant from charge-remote fragmentations, by heterolytic cleavages, giving structural information regarding the positions of functional groups (double bonds, hydroxy, epoxy and cyclopropane) in the oxidised PLPC, in a similar manner to what is described for lipids [37]. Thus, both isomers, namely 13,14-di-hydroxy-9,11-octadecadienoyl and 13-hydroperoxy-9,11-octadecadienoyl, may contribute as *sn*-2 residues linked to the 1-palmitoyl-3-glycerophosphatidylcholine in the peaks with rt 25 min. Other product ions observed at *m/z* 550.4 (a), 564.4 (b), 578.5 (c), 592.5 (d), 606.5 (e) and 620.5 (f) (Fig. 4b and Scheme 2), exhibit differences of 14 Da from each other and may be assigned to fragmentations occurring in the saturated moiety (alkyl chain) of the *sn*-2 residue (Table 2) by 1,4 hydrogen elimination mechanism [37], starting from the γ-bond of the ester group. These product ions are charge remote fragmentations typical of high-energy collisional activation although they have also been observed in the low-energy product ion spectra of short-chain phosphatidylcholines formed by radical peroxidation [38] and in triacylglycerols [37].

The LC–MS/MS spectrum obtained for the peak eluting at 18 min (Fig. 4a) exhibited the product ions at *m/z* 650.5 (−140 Da) and 690.5 (−100 Da), which may reflect the presence of the hydroxy at C-7 and the product ion at *m/z* 690.5 due to cleavage of C_{12}–C_{13} carbon bond indicating the presence of the 7,13-di-hydroxy-8,11-octadecadienoyl (Scheme 2C). On the other hand, both product ions (at *m/z* 650.5 and 690.5) may also be rationalised to the epoxy-hydroxy derivative (Scheme 2D), resulting from the cleavage in the vicinity of the epoxy group by a mechanism similar to the one proposed earlier for linoleic acid epoxy-peroxyl DMPO adducts [39]. This would suggest the

Table 2
Empirical formula, observed and calculated mass/charge ratios, double bond equivalents (DBE) and mass errors of the main fragments observed in the LC–MS/MS spectra for the ions resultant from the insertion of two oxygen atoms observed at *m/z* 788.6 and 790.6 with different retention times

$[MH]^+$	Predicted formula	Observed mass	Calculated mass	DBE	Error (mDa)	Error (ppm)
788.6						
rt 15.2 min	$C_{33}H_{65}NO_9P^+$	650.4373	650.4397	2.5	−2.4	−3.7
	$C_{35}H_{67}NO_9P^+$	676.4418	676.4553	3.5	−13.5	−20.0
rt 21.5 min	$C_{33}H_{65}NO_9P^+$	650.4269	650.4397	2.5	−12.8	−19.7
	$C_{36}H_{67}NO_9P^+$	688.4515	688.4553	4.5	−3.5	−5.2
790.6						
rt ∼18 min	$C_{33}H_{65}NO_9P^+$	650.4434	650.4397	2.5	3.7	5.7
	$C_{36}H_{69}NO_9P^+$	690.4764	690.4710	3.5	5.1	7.4
rt ∼25 min	$C_{27}H_{53}NO_8P^+$	550.3562	550.3509	2.5	5.3	9.7
	$C_{28}H_{55}NO_8P^+$	564.3689	564.3665	2.5	2.4	4.2
	$C_{29}H_{57}NO_8P^+$	578.3809	578.3822	2.5	−1.3	−2.2
	$C_{30}H_{59}NO_8P^+$	592.4060	592.3978	2.5	8.2	13.8
	$C_{31}H_{61}NO_8P^+$	606.4182	606.4135	2.5	4.7	7.8
	$C_{32}H_{63}NO_8P^+$	620.4213	620.4291	2.5	−7.8	−12.6
	$C_{36}H_{69}NO_8P^+$	674.4722	674.4761	3.5	−3.9	−5.8
	$C_{37}H_{69}NO_9P^+$	702.4681	702.4710	4.5	−2.9	−4.1

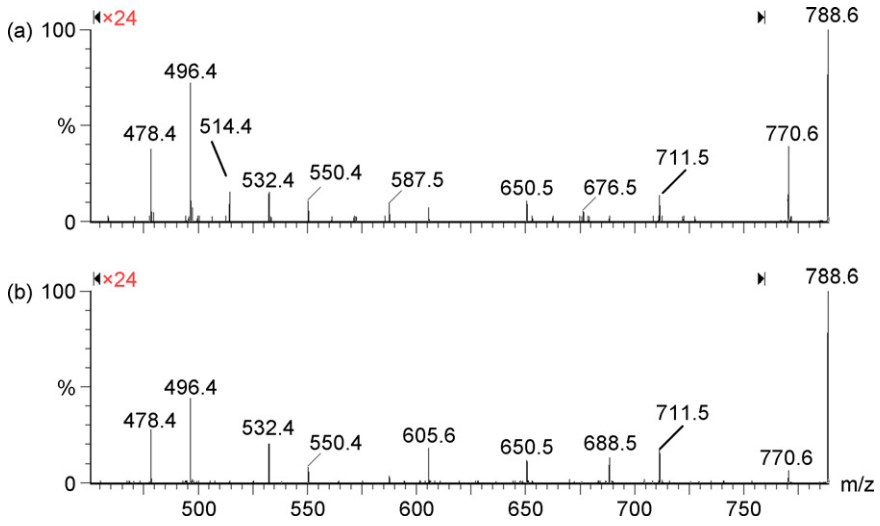

Fig. 5. LC–MS/MS spectra of $[MH]^+$ ion at *m/z* 788.6: (a) rt = 15.2 min and (b) rt = 21.5 min.

presence of the 13-hydroxy-9,10-epoxy-11-octadecenoyl as the *sn*-2 residue (Scheme 2D) attached to the phospholipid moiety. Thus, the product ions at *m/z* 650.5 and 690.5 may be originated from the fragmentation of the di-hydroxy (Scheme 2C) and/or the epoxy-hydroxy derivatives (Scheme 2D), although formed through different fragmentation pathways, exhibit the same elemental composition (observed with an error of 5.7 and 7.4 ppm, respectively; Table 2). The presence of epoxy-hydroxy derivatives as radical products of linoleic acid, as well as their degradation products, is described in the literature [40], and can thus be assumed to account for the ion at *m/z* 790.6 in oxidised PLPC. The peroxidation products proposed to occur in the two peaks, based on the LC–MS/MS data, are summarised in Table 2.

The RIC chromatogram of the ion at *m/z* 788.6, attributed to the keto-hydroxy and keto-epoxy derivatives, eluted in two with maxima at 15.2 and 21.5 min (Fig. 2b). The LC–MS/MS product ion spectra obtained in the different peaks (Fig. 5) showed common product ions at *m/z* 478.4 ($-R_2COOH$), 496.4 ($-R_2{=}C{=}O$), 532.4 ($-R_1COOH$), 550.4 ($-R_1{=}C{=}O$), 605.6 (−183 Da), 587.5 (−183 Da and H_2O), 711.6 (−59 Da and H_2O) and 770.6 ($-H_2O$). The presence of the product ion at *m/z* 650.5 ($-C_9H_{14}O$) originated from cleavage of the C_9–C_{10} bond, may suggest that the hydroxy is placed at C-9 (Scheme 3A), although the presence of the epoxy derivative can also be proposed (Scheme 3A1). The product ion at *m/z* 676.5 ($-C_7H_{12}O$) in Fig. 5a (rt 15.2 min) may be attributed to cleavage of the C_{11}–C_{12} denoting the presence of the keto group at C-9 and most probably with the hydroxy group at C-14 (Scheme 3B). The product ion observed at *m/z* 688.5 in Fig. 5b may result from cleavage of the C_{12}–C_{13} bond placing the keto group at C-10 with the hydroxy group at C-13 (Scheme 3C). In fact, these product ions are formed by cleavage of the γ-bond, earlier described as the asymmetrical cleavage in oxofatty acids [37]. On the other hand, as noted so far, the fragmentation which is governed by the functional

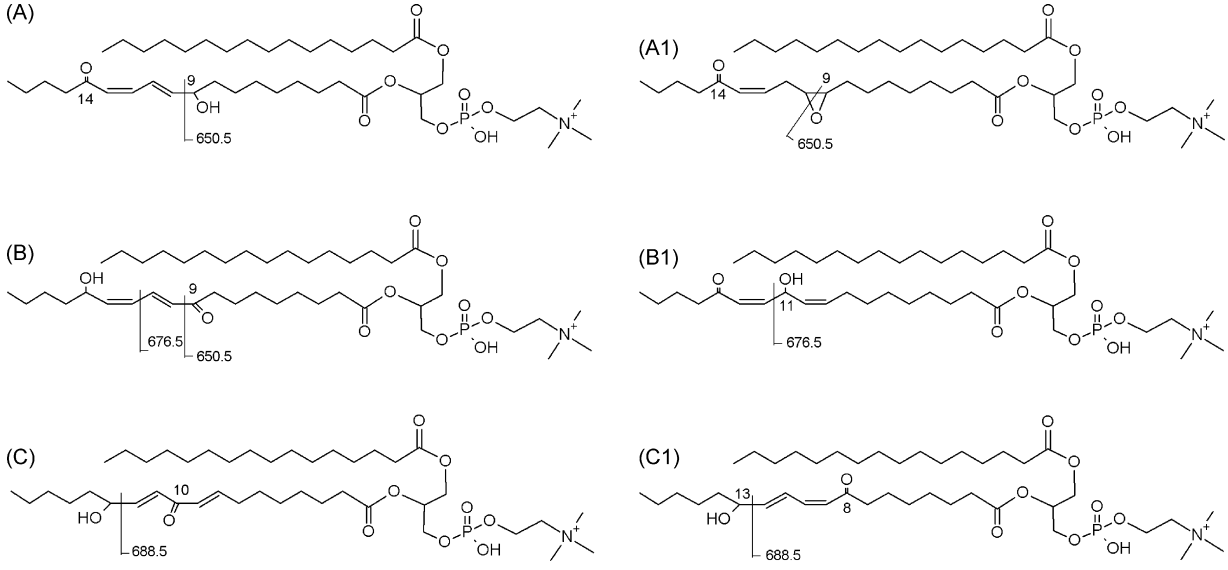

Scheme 3. Proposed structures contributing to the ion at *m/z* 788.6 showing the product ions formed by C–C cleavages.

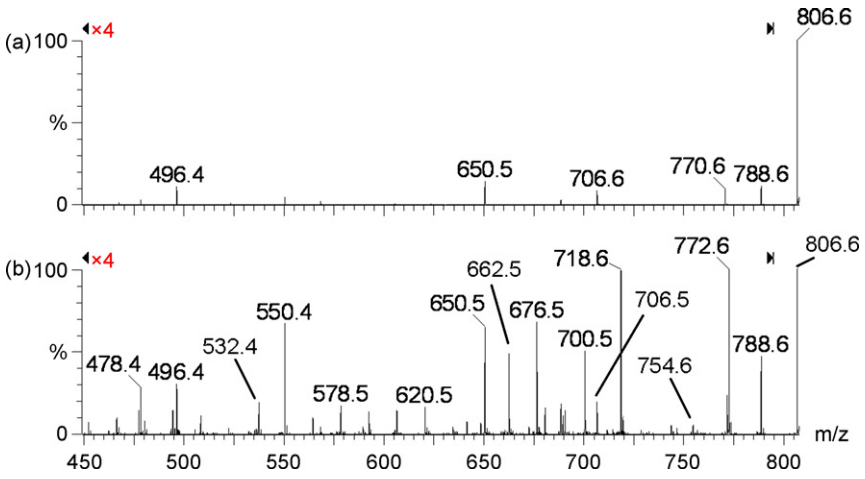

Fig. 6. LC–MS/MS spectra of $[MH]^+$ ion at *m/z* 806.6: (a) rt = 12.4 min and (b) rt = 18.8 min.

groups, in the case of keto-hydroxy derivatives, may be primarily dominated by the hydroxy group since the product ion spectra of keto derivatives (*m/z* 772.6, data not shown) exhibits no fragmentation, other than the one characteristic of glycerophosphatidylcholines. Thus, the product ion at *m/z* 650.5 suggests the hydroxy group at C-9 resulting from the 9-hydroxy-14-keto-10,12-octadecadienoyl (Scheme 3A), while the product ion at *m/z* 676.5 places the hydroxy group at C-11, suggesting the presence of the 11-hydroxy-14-keto-9,12-octadecadienoyl (Scheme 3B1). The product ion at *m/z* 688.5 ($-C_6H_{12}O$), with the structure $C_{36}H_{67}NO_9P^+$, determined with an experimental error of −3.5 mDa (−5.2 ppm; Table 2), places the hydroxy group at C-13 suggesting the 13-hydroxy-8-keto-9,11-octadecadienoyl (Scheme 3C1). All the structures proposed are feasible to occur as peroxidation products of lineloyl chain, and are in accordance with previous published results [14,40]. The peroxidation products proposed and identified based on the LC–MS/MS data are summarised in Table 4.

3.3. Peroxidation products with three oxygen atoms (*m/z* 806.6, 804.6 and 808.6)

The ion at *m/z* 806.6 (RIC on Fig. 1c), resultant from the insertion of three oxygen atoms in the unsaturated fatty acid chain, can be attributed to the hydroxy-hydroperoxy or to the tri-hydroxy derivatives. The ions observed at *m/z* 804.6 (RIC on Fig. 2c), may be attributed to the keto-di-hydroxy or to the keto-hydroperoxy, and the ion at *m/z* 808.6 (Fig. 2f) may be attributed to other tri-hydroxy derivatives by hydration of the epoxy-hydroxy derivatives, as suggested by Spiteller et al. [40].

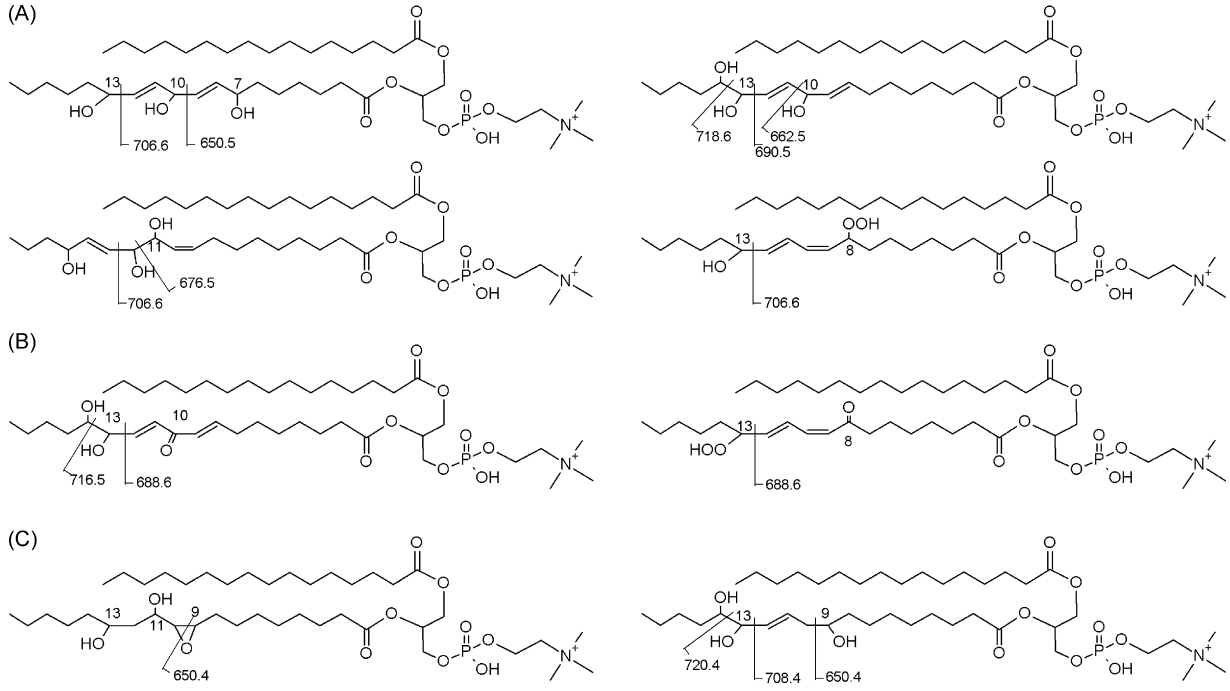

Scheme 4. Proposed structures contributing to the ions formed by insertion of three oxygen atoms with (A) *m/z* 806.6, (B) *m/z* 804.6 and (C) *m/z* 808.6, showing the product ions formed by C–C cleavages.

As can be observed, the tri-hydroxy (*m/z* 808.6) and the keto-hydroxy derivatives (*m/z* 804.6) exhibit different retention times (Figs. 1 and 2), corroborating that the keto derivatives are formed in solution during the radical peroxidation and not formed by dehydration phenomena due to in-source chemistry. The RIC chromatograms obtained for each of these ions showed maximum of elution at different retention times (Figs. 1 and 2), and in order to tentatively assign structures of PLPC peroxidation products the LC–MS/MS were obtained.

The LC–MS/MS spectra obtained for the ion at *m/z* 806.6, in the two maxima at 12.4 and 18.8 min (Fig. 1c), are depicted in Fig. 6. As can be seen, the main differences observed in the LC–MS/MS spectra are related with the major losses from the precursor ion, namely the loss of $2H_2O$ (*m/z* 770.6) and loss of $3H_2O$ (*m/z* 752.6) for the peak at 12.4 min (Fig. 6a) and the loss of H_2O_2 (*m/z* 772.6) and H_2O_2 with H_2O (*m/z* 754.6) for the peak at 18.8 min (Fig. 6b). Other product ions observed in the region of *m/z* 600–750, observed in Fig. 6a, at *m/z* 650.5 ($-C_9H_{16}O_2$) and 706.5 ($-C_6H_{12}O$), together with the previously described product ions at *m/z* 770.6 ($-2H_2O$) and 752.6 ($-3H_2O$), are consistent with the presence of the 7,10,13-tri-hydroxy-8,11-octadecadienoyl as *sn*-2 residue (Scheme 4A). The elemental composition determined for each product ion and the error associated are summarised in Table 3. The product ions observed in the LC–MS/MS mass spectrum of the peak eluting at 18.8 min (Fig. 6b) at *m/z* 718.6 ($-C_5H_{12}O$), 706.5 ($-C_6H_{12}O$), 676.5 ($-C_7H_{14}O_2$), 662.5 ($-C_8H_{16}O_2$) and 650.5 ($-C_9H_{16}O_2$), together with the product ion resulting from loss of 34 Da (*m/z* 772.6), suggest the presence of three different structures that can be attributed to the 13-hydroxy-8-hydroperoxy-9,11-octadecadienoyl, the 10,13,14-tri-hydroxy-9,11-octadecadienoyl, or also to the 11,12,15-tri-hydroxy-9,13-octadecadienoyl as *sn*-2 residues of PLPC (Scheme 4). The elemental composition determined for each product ion (Table 3) support the structures proposed. Product ions observed in Fig. 6b at *m/z* 550.4, 564.4, 578.4, 592.4, 606.4 and 620.4 (Table 2) are attributed to cleavages in the saturated alkyl moiety of the lineloyl chain. Particularly, the LC–MS/MS spectrum in Fig. 6a is very similar to the LC–MS/MS spectrum in Fig. 5b, which might suggest the occurrence of in-source dehydration reactions, but the LC–MS/MS spectra were acquired in different retention times. Based on the LC–MS/MS data here described, the ion at *m/z* 806.6 eluting in two peaks is composed of at least four different oxidation products, which are summarised in Table 4.

The ion at *m/z* 804.6 eluted in two major unresolved peaks with 15.2 and 15.8 min as can be seen by the RIC chromatogram obtained (Fig. 2c). The LC–MS/MS spectrum obtained for the unresolved peaks (Fig. 7) exhibited the product ions due to loss of H_2O_2 (*m/z* 770.6). The neutral losses of water and peroxide hydrogen observed from the precursor ion point out to the presence of keto-di-hydroxy derivative and keto-hydroperoxide derivatives to the RIC chromatogram of ion at *m/z* 804.6, although the contribution of epoxy-hydroxy-keto derivatives cannot be excluded. Still, some product ions, observed in Fig. 7b at *m/z* 730.6 (hydroxy at C-15), 716.5 (hydroxy group at C-14) allow proposing the substitutents in the higher carbon atoms, while in Fig. 7a the product ions at *m/z* 674.5 allow proposing the hydroperoxide group at C-13 and the 650.5 one hydroxy group at C-9. Overall,

Table 3
Empirical formula, observed and calculated mass/charge ratios, double bond equivalents (DBE) and mass errors of the main fragments observed in the LC–MS/MS spectra for the ions resultant from the insertion of three oxygen atoms observed at *m/z* 804.6, 806.6 and 808.6 with different retention times

$[MH]^+$	Predicted formula	Observed mass	Calculated mass	DBE	Error (mDa)	Error (ppm)
804.6						
rt 15.1 min	$C_{33}H_{65}NO_9P^+$	650.4387	650.4397	2.5	−1.0	−1.5
rt 15.8 min	$C_{36}H_{67}NO_9P^+$	688.4651	688.4553	4.5	9.8	14.2
	$C_{37}H_{69}NO_9P^+$	702.4719	702.4710	4.5	0.9	1.3
	$C_{37}H_{67}NO_{10}P^+$	716.4451	716.4503	5.5	−5.2	−7.2
	$C_{38}H_{69}NO_{10}P^+$	730.4677	730.4659	5.5	1.8	2.4
806.6						
rt 12.4 min	$C_{33}H_{65}NO_9P^+$	650.4377	650.4397	2.5	−2.0	−3.1
	$C_{36}H_{67}NO_9P^+$	688.4544	688.4553	4.5	−0.9	−1.4
	$C_{36}H_{69}NO_{10}P^+$	706.4673	706.4659	3.5	1.4	2.0
rt 18.8 min	$C_{33}H_{65}NO_9P^+$	650.4492	650.4397	2.5	9.5	14.6
	$C_{34}H_{65}NO_9P^+$	662.4463	662.4397	3.5	6.6	10.0
	$C_{35}H_{67}NO_9P^+$	676.4556	676.4553	3.5	0.3	0.4
	$C_{36}H_{67}NO_9P^+$	688.4553	688.4553	4.5	0.0	−0.1
	$C_{36}H_{69}NO_9P^+$	690.4729	690.4710	3.5	1.9	2.8
	$C_{36}H_{69}NO_{10}P^+$	706.4700	706.4659	3.5	4.1	5.8
	$C_{37}H_{69}NO_{10}P^+$	718.4677	718.4659	4.5	1.8	2.5
808.6						
rt 11.2 min	$C_{33}H_{65}NO_9P^+$	650.4472	650.4397	2.5	7.5	11.5
	$C_{36}H_{69}NO_9P^+$	690.4818	690.4710	3.5	10.8	15.6
rt 18.8 min	$C_{36}H_{71}NO_{10}P^+$	708.4875	708.4816	2.5	5.9	8.4
	$C_{37}H_{71}NO_{10}P^+$	720.4883	720.4816	3.5	6.7	9.4

Table 4
Retention times of the of the oxidised acyl fatty acid chains present as *sn*-2 acyl residues in oxidised PLPC identified based on the LC–MS/MS data

Retention time (min)	*m/z* value $[MH]^+$	Peroxidation product
11.2	808.6	1-Palmitoyl-2-(11,13-di-hydroxy-9,10-epoxy-octadecanoyl)-GPC
11.7	824.6	1-Palmitoyl-2-(9,12,13,14-tetra-hydroxy-10-octadecenoyl)-GPC
12.3	822.6	1-Palmitoyl-2-(7,10,14-tri-hydroxy-12,13-epoxy-8-octadecenoyl)-GPC
12.4	806.6	1-Palmitoyl-2-(7,10,13-tri-hydroxy-8,11-octadecadienoyl)-GPC
15.4	804.6	1-Palmitoyl-2-(14,15-di-hydroxy-9-keto-10,12-octadecadienoyl)-GPC
15.2	822.6	1-Palmitoyl-2-(8,13-di-hydroxy-14-hydroperoxy-9,11-octadecadienoyl)-GPC
15.2	822.6	1-Palmitoyl-2-(9,10,11-tri-hydroxy-14-keto-12-octadecenoyl)-GPC
15.2	788.6	1-Palmitoyl-2-(9,10-epoxy-14-keto-12-octadecenoyl)-GPC
15.9	804.6	1-Palmitoyl-2-(13,14-di-hydroxy-10-keto-8,11-octadecadienoyl)-GPC
15.9	804.6	1-Palmitoyl-2-(13-hydroperoxy-8-keto-9,11-octadecadienoyl)-GPC
17.8–18.7	790.6	1-Palmitoyl-2-(7,13-di-hydroxy-8,11-octadecadienoyl)-GPC
17.8–18.7	790.6	1-Palmitoyl-2-(13-hydroxy-9,10-epoxy-11-octadecenoyl)-GPC
18.8	806.6	1-Palmitoyl-2-(13-hydroxy-8-hydroperoxy-9,11-octadecadienoyl)-GPC
18.8	806.6	1-Palmitoyl-2-(10,13,14-tri-hydroxy-9,11-octadecadienoyl)-GPC
18.8	806.6	1-Palmitoyl-2-(11,12,15-tri-hydroxy-9,13-octadecadienoyl)-GPC
18.8	808.6	1-Palmitoyl-2-(9,13,14-tri-hydroxy-11-octadecenoyl)-GPC
19.3	822.6	1-Palmitoyl-2-(9,12-di-hydroxy-15-hydroperoxy-10,13-octadecadienoyl)-GPC
19.3	822.6	1-Palmitoyl-2-(8,9,10-tri-hydroxy-13-keto-10-octadecenoyl)-GPC
21.5	788.6	1-Palmitoyl-2-(9-hydroxy-14-keto-10,12-octadecadienoyl)-GPC
21.5	788.6	1-Palmitoyl-2-(11-hydroxy-14-keto-9,12-octadecadienoyl)-GPC
21.5	788.6	1-Palmitoyl-2-(13-hydroxy-8-keto-9,11-octadecadienoyl)-GPC
24.4–25.4	790.6	1-Palmitoyl-2-(13,14-di-hydroxy-9,11-octadecadienoyl)-GPC
24.4–25.4	790.6	1-Palmitoyl-2-(13-hydroperoxy-9,11-octadecadienoyl)-GPC
24–25	774.6	1-Palmitoyl-2-(9,10-epoxy-10,12-octadecadienoyl)-GPC
25.4	772.6	1-Palmitoyl-2-(9-keto-10,12-octadecadienoyl)-GPC
31.1	774.6	1-Palmitoyl-2-(9-hydroxy-10,12-octadecadienoyl)-GPC
31.1	774.6	1-Palmitoyl-2-(10-hydroxy-8,11-octadecadienoyl)-GPC
31.1	774.6	1-Palmitoyl-2-(12-hydroxy-10,13-octadecadienoyl)-GPC
31.1	774.6	1-Palmitoyl-2-(13-hydroxy-9,11-octadecadienoyl)-GPC

GPC: glycero-3-phosphocholine.

based on the product ions observed it is suggested the presence of the 13,14-di-hydroxy-10-keto-8,11-octadecadienoyl or the 13-hydroperoxide-8-keto-9,11-octadecadienoyl, and the 14,15-di-hydroxy-9-keto-10,12-octadecadienoyl. The elemental composition determined for each product ion is shown in Table 3, and support the proposed structures (Table 4).

The RIC for the ion at *m/z* 808.6 (Fig. 2f) showed elution in two well resolved peaks with maxima of elution at 11.2 and 18.8 min. The ion at *m/z* 808.6 is consistent with the presence of a tri-hydroxy derivative with only one double bond instead of two double bonds as was depicted for the ion at *m/z* 806.6. In fact, the LC–MS/MS spectra obtained for the ion with rt 11.2 min (data not shown) exhibited the product ions at *m/z* 790.5 ($-H_2O$), 772.5 ($-2H_2O$) and 552 ($-R_1COOH$), which indicated the oxygen atoms to be placed at the *sn*-2 residue. Other product ions at *m/z* 650.4, with the structure $C_{33}H_{65}NO_9P^+$ (Table 3), resulted from cleavage between C_9–C_{10} carbon bond, and at *m/z* 690.5, with the structure $C_{36}H_{69}NO_9P^+$ (Table 3), resulted from cleavage between C_{12}–C_{13}, allow proposing the contribution of the 11,13-di-hydroxy-9,10-epoxy-octadecanoyl as the *sn*-2 acyl residue (Scheme 4C), while the LC–MS/MS obtained for the ion with rt 18.8 min (data not shown) exhibited the product ions at *m/z* 790.5 ($-H_2O$) and 774.5 ($-H_2O_2$) by a combined homolytic cleavage between two hydroxy groups in vicinal positions, and at *m/z* 720.5 ($-C_5H_{12}O$) by cleavage of C_{13}–C_{14} linkage suggesting the presence of an oxygen atom at C-14 (Table 3). Product ion present with minor relative abundance at *m/z* 708.4, resultant from cleavages in the vicinity of the double bond or the hydroxy groups suggest the presence of the 9,13,14-tri-hydroxy-11-octadecenoyl (Scheme 4C) as the *sn*-2 residue. More recently, in a study aimed at the identification of enzymatic extracts of diacyl-phosphatidylcholines isolated from rat heart tissue, the ion at *m/z* 808.6 was attributed to the tri-hydroxy PLPC derivative based on the loss of one, two and three water molecules, although information regarding the location of the hydroxy groups was not suggested [26]. The presence of tri-hydroxy derivatives of the linoleic acid bearing vicinal hydroxy groups was earlier proposed as linoleic peroxidation products formed by hydrolysis of the epoxy-hydroxy linoleic acid derivatives [40], and also as peroxidation products in cardiolipin–cytochrome *c* system [41].

3.4. Peroxidation products with four oxygen atoms (m/z 822.6 and 824.6)

The RIC chromatogram obtained for the ion at *m/z* 822.5 (Fig. 1e) shows the elution of oxidation products in five peaks with rt 12.3, 13.8, 14.3, 15.2 and 19.3 min suggesting the elution of several structural and positional isomers. The LC–MS/MS spectra obtained in each peak (data not shown) exhibit, apart from the product ions at *m/z* 184.1, 478.4 and 496.4, the product ions formed by loss of H_2O, of H_2O_2 and of both combined, as is the case of product ions at *m/z* 804.5 ($-H_2O$), 788.5 ($-H_2O_2$), 786.5 ($-2H_2O$), 770.5 ($-H_2O_2$ and H_2O) and 768.5 ($-3H_2O$).

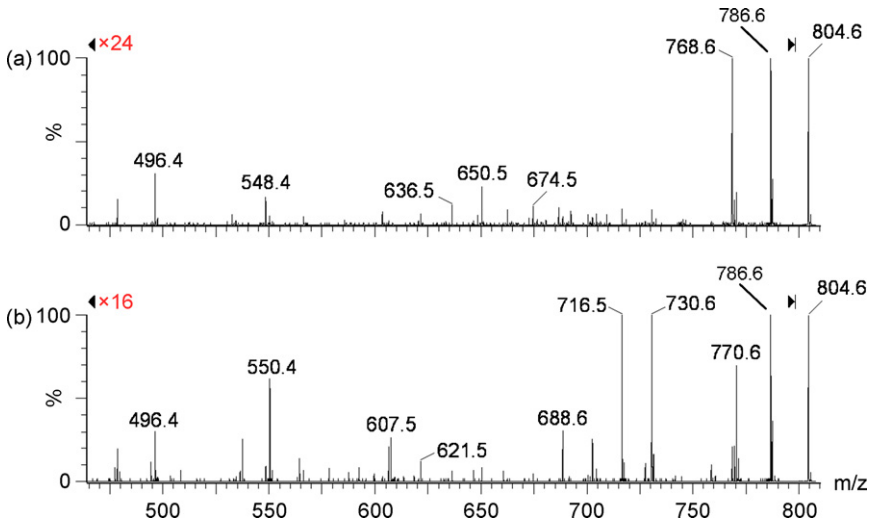

Fig. 7. LC–MS/MS spectra of $[MH]^+$ ion at *m/z* 804.6 with rt = 15–16 min.

However, the low ion current of peaks with rt 13.8 and 14.3 min, hampered the acquisition of the LC–MS/MS spectra, and the LC–MS/MS spectra for the remaining peaks of the ion at *m/z* 822.5 are shown in Fig. 8a–c. The product ion observed at *m/z* 754.5 (Fig. 8b and c), in particular, may be due to either combined loss of $2H_2O_2$ or, to combined loss of $2H_2O$ with O_2, since the product ion at *m/z* 786.5 ($-2H_2O$) is also observed in the LC–MS/MS spectra (Fig. 8b). The loss of the oxygen molecule may occur by a mechanism similar to what was earlier proposed suggesting the presence of a conjugated hydroperoxide derivative [18]. Due to the wide variety possible isomers (structural and positional) generated by the insertion of high number of oxygen atoms into the *sn*-2 acyl chain (lineloyl), co-elution of different structures takes place.

The LC–MS/MS spectrum obtained for the ion at *m/z* 822.5 with the peak maximum at 12.3 min (Fig. 8a) showed the product ions at *m/z* 650.4, 704.4 and 732.4 that may suggest the contribution of the 7,10,14-tri-hydroxy-12,13-epoxy-8-octadecenoyl as the *sn*-2 residue derivative (Scheme 5A), which is also consistent with the observed loss of $3H_2O$ (*m/z* 768.6). The product ions observed for the peak at 15.2 min (Fig. 8b) at *m/z* 636.4, 718.4, 788.5 and the product ion at *m/z* 754.6 (loss $2H_2O$ and O_2), may account for the presence of 8,13-di-hydroxy-14-hydroperoxy-9,11-octadecadienoyl acid (Scheme 5B). On the other hand, the contribution of 9,10,11-tri-hydroxy-14-keto-12-octadecenoyl (Scheme 5C) also supports the observation of the product ions at *m/z* 650.4 and 738.4 and the loss of 34 Da observed from the precursor ion, and in turn may account for the presence of the product ion at *m/z* 704.5 due to loss of 34 Da combined with the cleavage between C_{13}–C_{14}. The 8,9,10-tri-hydroxy-13-keto-10-octadecenoyl (Scheme 5D) and the 9,12-di-hydroxy-15-hydroperoxy-10,13-octadecadienoyl derivatives (Scheme 5E) allow rationalising the product ions at *m/z* 650.4, 662.4, 696.4 and 706.4, and the loss of one H_2O_2 (−34 Da) observed for the maximum rt with 19.3 min (Fig. 8c). By plotting the RIC chromatogram of the product ions with *m/z* 636.4, 650.4, 662.4, 696.4, 704.4, 706.4, 718.4 and 738.4 used for structural characterisation of ion at *m/z* 822.5 (data not shown) it is possi-

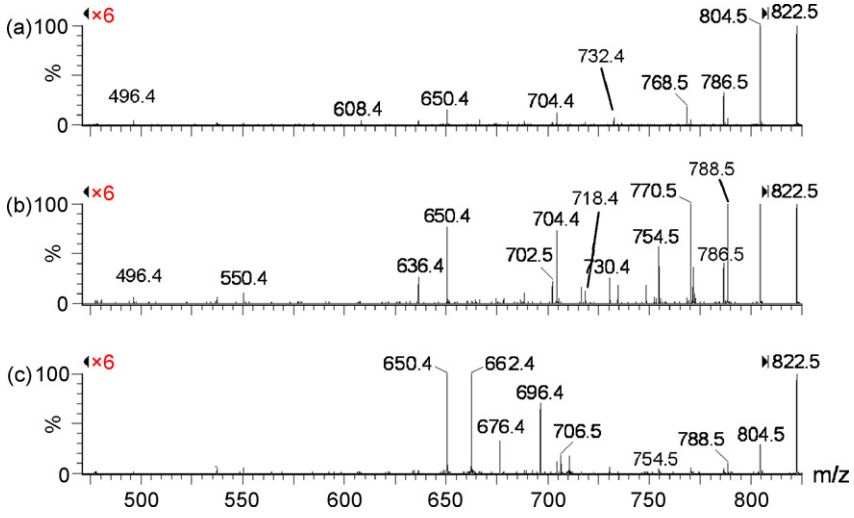

Fig. 8. LC–MS/MS spectra of $[MH]^+$ ion at *m/z* 822.6: (a) rt = 12.3 min, (b) rt = 15.2 min and (c) rt = 19.3 min.

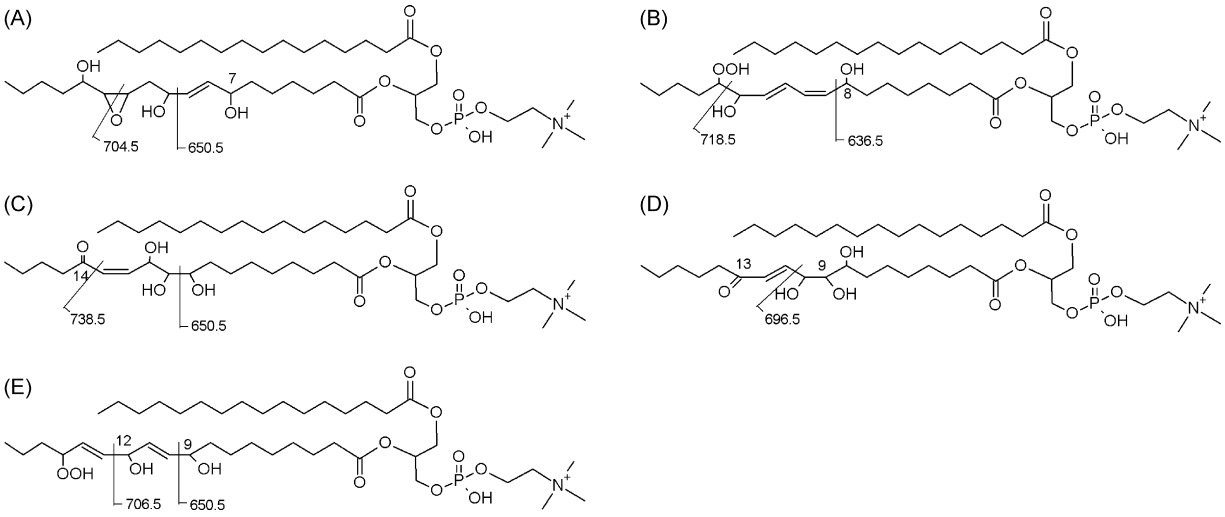

Scheme 5. Proposed structures contributing to the ion at *m/z* 822.5 (insertion of four oxygen atoms) showing the product ions formed by C–C cleavages.

ble to group the product ions according to the differences in the retention times observed corroborating the elution of different PLPC oxidation products. The elemental composition determined for each product ion observed in the LC–MS/MS spectra and the errors associated were calculated (data not shown) and the identification was accepted when mass errors were inferior to 25 ppm. The peroxidation products identified based on the LC–MS/MS data are summarised in Table 4. Bearing in mind the results here described it is, therefore, feasible to assume that the presence of unresolved peaks seen in the RIC chromatograms of the several ions studied is the result of the considerable heterogeneity of the oxidised *sn*-2 acyl chains that may arise from radical oxidation of the linoleic acid moiety in PLPC.

The product ion spectrum obtained for the ion at *m/z* 824.6 (data not shown) eluting with rt 11.7 min (Fig. 2) exhibited the typical product ions (–R_1COOH and –R_2COOH), the product ions due to loss of water and hydrogen peroxide, *m/z* 806.6 (–H_2O), 790.6 (–2H_2O), 788.6 (–H_2O_2) and 772.6 (–H_2O–H_2O_2) from the precursor ion, and others at *m/z* 650.4 (cleavage C_9–C_{10}), 706.4 (cleavage C_{12}–C_{13}) and 736.5 (cleavage C_{13}–C_{14}) showing errors of 15.5, 7.2 and 2.1 ppm, respectively, for the proposed structures (data not shown). These product ions were consistent with the contribution of the 9,12,13,14-tetra-hydroxy-10-octadecenoyl as the *sn*-2 acyl residue to the relative abundance of the ion at *m/z* 824.6.

Other ions that may also result from the insertion of four oxygen atoms (*m/z* 820.6), five oxygen atoms (*m/z* 836.6 and 840.6) and six oxygen atoms (*m/z* 854.6), were also formed as can be seen by their RIC chromatograms (Fig. 2). All the ions exhibited different retention times, suggesting that were in fact different peroxidation products formed during the radical reaction of PLPC. However, the acquisition of the LC–MS/MS spectra of these ions in the different chromatographic peaks was, limited by the low ion current obtained for these ions, constraining our ability to perform structural characterisation. Nevertheless, the presence of peroxidation products with high number of oxygen atoms may be responsible for the increase of the hydrophilic character described for membrane bilayers [5,6]. The identification of these products suggests that the hydroxyl radical was able to penetrate into the lipophilic packing of the liposomes and thus initiate/propagate the radical reaction. In fact, Vitrac et al. [19], through light-scattering studies, have concluded that approximately 90% of PLPC vesicles were of low diameter, when formed during sonication [19]. The occurrence of a phospholipid dispersion comprised of low-diameter vesicles would contain highly curved surface and, therefore, a looser packing of the lipid chains facilitating ROS penetration [42].

In the case of LC–MS/MS analysis of long-chain PLPC products, among the isomers identified several contained the C-9 position substituted, which suggests this carbon atom to be easily oxidised or the oxidation product to be very stable. Remarkably, the identification of short-chain product with *m/z* 650.4 assigned to 1-palmitoyl-2-(9-oxo-nonanoyl)-glycerophosphocholine and observed during the LC–MS analysis of radical oxidised PLPC liposomes [25] and in oxidised LDL [14,15] was found to be one of the predominant PLPC short-chain products. The phospholipid short-chain products containing the carbonyl moieties are increasingly being studied in an attempt to determine their role on the uptake of oxidised LDL by macrophages [43] or the role of phospholipid–peptide interactions in the initial events of apoptosis observed in endothelial cultured cells [44].

Under the LC–MS conditions used in this study for the separation of PLPC peroxidation products, it was possible to propose the presence of structural, positional and geometrical isomers of PLPC long-chain oxidation products formed under Fenton conditions. In a recent study, several phosphatidylcholine oxidation products formed under enzymatic conditions (lipoxygenase) were proposed [26], and although the proposed peroxidation products were not fully characterised, to the products may be more structurally homogenous due to the specificity of the enzymatic oxidation reaction (lipoxygenase) [45]. As pointed out in this study, detailed structural information about the structure can be obtained based on the MS/MS data using the product ions (i) due to loss of H_2O and H_2O_2 from the precursor ion, (ii) due to loss of R_1COOH and R_2COOH (lyso-phosphatidylcholine product ions) give information about the oxidised acyl chain,

and (iii) due to loss of alkene and aldehyde moieties resulting from charge remote fragmentations in the unsaturated backbone.

Based on the peroxidation products here described, the polyhydroxy derivatives identified as *sn*-2 acyl derivatives in oxidised PLPC, either with hydroxy groups in vicinal positions or in distant positions, are apparently predominant over the hydroperoxide derivatives. These results suggest that radical oxidation of diacyl-GPC under the Fenton conditions, the hydroxy derivatives appear to be more stable, or its formation more favourable. In *in vivo* conditions, the presence glutathione peroxidases (GPx), which are described to reduce the hydroperoxides to their hydroxy derivatives [3,46], may also lead to the predominance of hydroxy derivatives over hydroperoxides, formed either through enzymatic or non-enzymatic pathways. Also, in *in vivo* conditions the formation of phospholipid peroxidation products, which is promoted not only by ROS but also by enzymatic reactions, may enhance or promote the presence of some phospholipid peroxidation products over others, which in turn might simplify the composition of the oxidised phospholipids and thus facilitating their identification in a complex mixture from biological samples. On the other hand, using only one phospholipid several isomeric and positional isomers were identified in this study, thus it is expected that the identification of radical peroxidation products in biological samples may turn out to be a more challenging task considering that ω-3, ω-6 and ω-9 fatty acids are present in biological membranes [47]. In summary, the PLPC peroxidation products identified based on these fragmentation pathways might create the bases for widening the products monitored in biological samples, such as those reported in oxLDL as potential biomarkers.

In the overall, the structural changes that take place in membrane phospholipids, either with formation of long-chain products or of the short-chain products, with terminal aldehyde and carboxylic groups [25], that may account for the described decrease of membrane packing and increase of membrane disorder [5,6], may further promote ROS penetration and the propagation of the damage, with consequences to the membrane bilayer shape and in the diffusion capacity of red blood cells with major implications in tissue oxygenation. Propagation of the oxidative damage may induce to the loss of membrane integrity, essential for proper phospholipid–phospholipid and protein–phospholipid interactions [9].

4. Conclusions

Tandem mass spectrometry (MS/MS) together with reverse-phase chromatography was used for the differentiation of oxidised PLPC products formed *in vitro* under non-enzymatic oxidative conditions. The LC–MS conditions used allowed the separation of the different isomers obtained for the oxidation products with the same *m*/*z* value and the LC–MS/MS provided the structural identification for each of the products. The different product ions observed in the LC–MS/MS spectra were interpreted as resulting to loss of aldehyde and alkene moieties corresponding to charge remote fragmentations. These fragmentations together with the product ions due to loss of water and hydrogen peroxide from the precursor ions allowed establishing the different structural features of PLPC long-chain peroxidation products. These structural features were determined in peroxidation products containing one to five oxygen atoms, which included keto, hydroxy, epoxy, keto-hydroxy, hydroperoxide, di-hydroxy, keto-hydroperoxide, keto-di-hydroxy, hydroxy-hydroperoxide and tri-hydroxy derivatives of PLPC. These data shows the separation and identification of structural and positional isomers of oxidised phosphatidylcholine.

Acknowledgements

The authors gratefully acknowledge the financial support provided to Ana Reis (Ph.D. grant SFRH/BD/10358/2002) by the Foundation for Science and Technology (FCT) and FSE (III Quadro Comunitário de Apoio).

References

[1] J. Pincemail, in: A.E. Favier, J. Cadet, B. Kalyanaraman, M. Fontecave, J.L. Pierre (Eds.), Analysis of Free Radicals in Biological Systems, Verlag, Berlin, 1995, p. 83.
[2] G. Spiteller, Chem. Phys. Lipids 95 (1998) 105.
[3] A. Girotti, J. Lipid Res. 39 (1998) 1529.
[4] J.W. Borst, N.V. Visser, O. Kouptsova, A.J.W.G. Visser, Biochim. Biophys. Acta 1487 (2000) 61.
[5] F.M. Megli, K. Sabatini, Chem. Phys. Lipids 125 (2003) 161.
[6] F.M. Megli, K. Sabatini, FEBS Lett. 573 (2004) 68.
[7] M. Carini, G. Aldini, R.M. Facino, Mass Spectrom. Rev. 23 (2004) 281.
[8] A. Reis, P. Domingues, A.J. Ferrer-Correia, M.R.M. Domingues, J. Am. Soc. Mass Spectrom. 17 (2006) 657.
[9] F. van Voorst, B. de Kruijff, Biochem. J. 347 (2000) 601.
[10] T.M. McIntyre, G.A. Zimmerman, S.M. Prescott, J. Biol. Chem. 274 (1999) 25189.
[11] C.E. Clay, A.M. Namen, G.-I. Atsumi, M.C. Willingham, K.P. High, T.E. Kute, A.J. Trimboli, A.N. Fonteh, P.A. Dawson, F.H. Chilton, Carcinogenesis 20 (1999) 1905.
[12] S.J. Shelley, H.-Y.J. Wang, A.S. Woods, J. Am. Soc. Mass Spectrom. 16 (2005) 2052.
[13] D.Y. Bang, D. Kang, M.H. Moon, J. Chromatogr. A 1104 (2006) 222.
[14] H. Itabe, H. Yamamoto, M. Suzuki, Y. Kawai, Y. Nakagwa, A. Suzuki, T. Imanaka, T. Takano, J. Biol. Chem. 271 (1996) 33208.
[15] G.K. Marathe, K.A. Harrison, R.C. Murphy, S.M. Prescott, G.A. Zimmerman, T.M. McIntyre, Free Radic. Biol. Med. 28 (2000) 1762.
[16] E.A. Podrez, E. Poliakov, Z. Shen, R. Zhang, Y. Deng, M. Sun, P.J. Finton, L. Shan, B. Gugiu, P.L. Fox, H.F. Hoff, R.G. Salomon, S.L. Hazen, J. Biol. Chem. 277 (2002) 38503.
[17] J.-R. Zhang, A.R. Cazers, B.S. Lutzke, E.D. Hall, Free Radic. Biol. Med. 18 (1995) 1.
[18] A. Reis, P. Domingues, A.J. Ferrer-Correia, M.R.M. Domingues, J. Mass Spectrom. 39 (2004) 1513.
[19] H. Vitrac, M. Courrègelongue, M. Couturier, F. Collin, P. Thérond, S. Rémita, P. Peretti, D. Jore, M. Gardès-Albert, Can. J. Physiol. Pharmacol. 82 (2004) 153.
[20] J. Adachi, N. Yoshida, R. Funae, H. Nushida, M. Asano, Y. Ueno, J. Chromatogr. B 806 (2004) 41.
[21] P. Wheelan, J.A. Zirrolli, R.C. Murphy, J. Am. Soc. Mass Spectrom. 7 (1996) 140.
[22] T. Nakamura, D.L. Bratton, R.C. Murphy, J. Mass Spectrom. 32 (1997) 888.
[23] D.K. MacMillan, R.C. Murphy, J. Am. Soc. Mass Spectrom. 6 (1995) 1190.
[24] K.A. Harrison, R.C. Murphy, J. Biol. Chem. 270 (1995) 17273.
[25] A. Reis, M.R.M. Domingues, F.M.L. Amado, A.J. Ferrer-Correia, P. Domingues, Biomed. Chromatogr. 19 (2005) 129.

[26] J. Adachi, N. Yoshida, M. Sato, K. Nakagawa, Y. Yamamoto, Y. Ueno, J. Chromatogr. B 823 (2005) 37.
[27] M. Inouye, T. Moi, K. Sumino, Biochim. Biophys. Acta 1438 (1999) 204.
[28] J. Adachi, S. Matsushita, N. Yoshioka, R. Funae, T. Fujita, S. Higuchi, Y. Ueno, J. Lipid Res. 45 (2004) 967.
[29] J. Folch, M. Lees, G.H.S. Stanley, J. Biol. Chem. 226 (1957) 497.
[30] O. Sergent, I. Morel, J. Cillard, in: A. Sigel, H. Sigel (Eds.), Metal Ions in Biological Systems, vol. 36, Marcel Dekker, Inc., New York, 1999, p. 251.
[31] N. Pelizzi, S. Catinella, S. Barboso, M. Zanol, Rapid Commun. Mass Spectrom. 16 (2002) 2215.
[32] F.-F. Hsu, J. Turk, J. Am. Soc. Mass Spectrom. 14 (2003) 352.
[33] F.-F. Hsu, J. Turk, J. Am. Soc. Mass Spectrom. 10 (1999) 600.
[34] L.M. Hall, R.C. Murphy, J. Am. Soc. Mass Spectrom. 9 (1998) 527.
[35] F.A. Fitzpatrick, D.R. Morton, M.A. Wynalda, J. Biol. Chem. 257 (1982) 4680.
[36] F. Giuffrida, F. Destaillats, L.H. Skibsted, F. Dionisi, Chem. Phys. Lipids 131 (2004) 41.
[37] C. Cheng, M.L. Gross, Mass Spectrom. Rev. 19 (2000) 398.
[38] A. Reis, P. Domingues, A.J. Ferrer-Correia, M.R.M. Domingues, Rapid Commun. Mass Spectrom. 18 (2004) 2849.
[39] A. Reis, M.R.M. Domingues, F.M.L. Amado, A.J. Ferrer-Correia, P. Domingues, J. Am. Soc. Mass Spectrom. 14 (2003) 1250.
[40] P. Spiteller, W. Kern, J. Reiner, G. Spiteller, Biochim. Biophys. Acta 1531 (2001) 188.
[41] H. Iwase, T. Talatori, M. Nagao, H. Nijima, K. Iwadate, Y. Matsuda, M. Kobayashi, Free Radic. Biol. Med. 24 (1998) 1492.
[42] Q.-T. Li, M.H. Yeo, B.K. Tan, Biochem. Biophys. Res. Commun. 273 (2000) 72.
[43] C.J. Brame, O. Boutaud, S.S. Davies, T. Yang, J.A. Oates, D. Roden, L.J. Roberts II, J. Biol. Chem. 279 (2004) 13447.
[44] G. Subbanagounder, Y. Deng, C. Borromeo, A.N. Dooley, J.A. Berliner, R.G. Salomon, Vasc. Pharmacol. 38 (2002) 201.
[45] H. Kitaguchi, K. Ohkubo, S. Ogo, S. Fukuzumi, J. Am. Soc. Mass Spectrom. 127 (2005) 6605.
[46] E. Niki, Y. Yoshida, Y. Saito, N. Nguchi, Biochem. Biophys. Res. Commun. 338 (2005) 668.
[47] M.A. Yorek, in: C. Gregor (Ed.), Phospholipids Handbook, Marcel Dekker, New York, 1993, p. 745.